Evaluation of poloidal distribution from edge impurity emissions measured at different toroidal positions in Large Helical Device

H. M. Zhang[1], S. Morita[1,2], T. Ohishi[1,2], M. Kobayashi[1,2], M. Goto[1,2] and X. L. Huang[1]

[1]Graduate University for Advanced Studies, Toki 509-5292, Gifu, Japan

[2]National Institute for Fusion Science, Toki 509-5292, Gifu, Japan

Abstract

Two-dimensional (2-D) distribution of edge impurity line emissions has been measured for CIV, CVI, FeXV and FeXVIII using a space-resolved extreme ultraviolet (EUV) spectrometer in Large Helical Device (LHD). A strong emission trajectory along the plasma boundary is observed at the top and the bottom edges in the 2-D distribution. The poloidal distribution of impurity emissivity has been evaluated by analyzing the 2-D distribution against magnetic surfaces calculated with a 3-D equilibrium code, VMEC. Inner and outer boundaries of the edge impurity location are estimated by analyzing each vertical emission profile measured at different toroidal positions. The observation chord length passing through an emission contour is calculated based on the radial thickness of the impurity emission location. The poloidal distribution of CIV, CVI, FeXV and FeXVIII with different ionization energies is thus reconstructed from the 2-D distribution. A non-uniform poloidal distribution is clearly observed for all these impurity species located different plasma radii. It is experimentally confirmed that the poloidal distribution becomes gradually uniform as the radial location of impurity ions moves from the ergodic layer to the plasma core. The non-uniform poloidal distribution of CIV emissivity is also confirmed by the simulation with a 3-D edge transport code, EMC3-EIRENE.

1. Introduction

In LHD, the core plasma is surrounded by the ergodic layer, in which magnetic fields with a three-dimensional (3-D) structure are formed by higher order components in magnetic fields created with a pair of helical coils and by overlapping of edge small islands [1-3]. A 2-D space-resolved EUV spectrometer system has been developed to measure the 2-D distribution of impurity line emissions in the ergodic layer [4]. The 2-D distribution of edge impurity emissions has been measured for various impurity species, e.g. CIV, HeII and FeXVI [4,5]. An entirely non-uniform 2-D distribution has been observed for such edge impurity emissions. These impurity emissions are enhanced at the top and bottom plasma boundaries and in the vicinity of X-points. The 2-D distribution measured here may reflect a non-uniform poloidal distribution in the edge impurity emission. Therefore, it is important to evaluate the poloidal distribution of edge impurity emissions for gaining a deeper understanding of the impurity behavior in the plasma edge, in particular, in the ergodic layer. Since the LHD plasma shape poloidally rotates five times during one toroidal turn, the poloidal distribution of edge impurity emissions can be estimated from 2-D distributions. In practice, the poloidal distribution of impurity emissivity is obtained by analyzing each vertical profile measured at different toroidal positions. In this paper, the poloidal impurity distribution is presented for CIV, CVI, FeXV and FeXVIII with different ionization energies. The result is compared with simulation with the EMC3-EIRENE code.

2. EUV spectrometer and 2-D distribution measurement

A 2-D space-resolved EUV spectrometer has been developed to measure the 2-D distribution of impurity emissions in the wavelength range of 60–400 Å by horizontally scanning optical axis of the spectrometer [4]. The horizontal view of LHD plasmas with ergodic layer is shown in Fig. 1. The LHD port is denoted with diamond a solid line. The observation range of 2-D distribution measurement is then limited by 120cm and 90cm in vertical and horizontal directions, respectively. Inboard and outboard X-point trajectories are denoted with dotted and dashed lines, respectively.

The 2-D distribution of impurity emissions is shown in Fig. 2 for CIV (384.174 Å, E_i = 64.0 eV), CVI (2 × 33.73 Å, 490.0 eV), FeXV (284.164 Å, 456.2 eV) and FeXVIII (93.92 Å, 1357.8 eV) in low-density (n_e~1x10^{13}cm^{-3}) ICRF discharges with magnetic axis position of R_{ax} = 3.60 m. The intensity of impurity line emissions is absolutely calibrated using radial profiles of bremsstrahlung continuum in EUV and visible ranges [6]. In the 2-D distribution emissions near the top and the bottom plasma boundaries are enhanced due to a long chord length passing through the edge plasma. The inboard X-point trajectory (see Fig. 1) is also enhanced for CIV and CVI indicating a non-uniform poloidal distribution to line emissions in the ergodic layer.

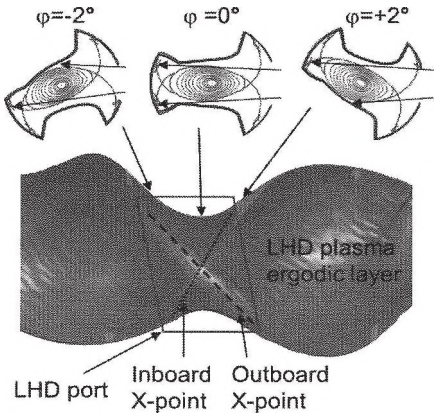

Fig. 1 Horizontal view of LHD ergodic layer and poloidal plasma cross sections at three different toroidal angles of φ = − 2°, 0° and + 2°.

3. Analysis of poloidal distribution

The elliptical cross section of LHD plasmas within the observation range is shown in Fig. 1 at three different toroidal positions of φ=-2°, 0° and +2°. The observation chord passing through the top and the bottom plasma boundaries are also indicated with two solid arrows in each poloidal cross section. In the figure it is clear that the emission intensity in the top and the bottom edges measured at different toroidal positions can express information on the poloidal distribution of impurity emissions. Then, an evaluation of the poloidal distribution of edge impurity emissions is attempted by analyzing the impurity emission at the top and the bottom edges in the 2-D distribution. In the analysis data from X-points with extremely non-uniform emissions are not used.

As the first step, the magnetic flux surface of LHD is calculated with a 3-D equilibrium code, VMEC, as a function of pressure profile. Although no magnetic surface exists in the ergodic layer, virtual magnetic surfaces are assumed at ρ > 1, which are calculated by extrapolating the magnetic flux surface at last closed flux surface (LCFS). This assumption is usually used in LHD when an edge plasma in the ergodic layer is analyzed.

An example of the vertical profile of impurity emissions at the top edge is shown in Fig. 3 for CIV measured at Y = 0, which means φ=0° (see Fig. 2). A sharp peak is observed near the plasma edge boundary. Here, inner and outer boundaries of the impurity vertical profile are defined by intensities at the peak and the half maximum, respectively. In the figure, then, the inner and outer boundaries of CIV radial profiles are estimated to be ρ = 1.02 and ρ = 1.06, respectively.

After analyzing the inner and outer boundaries of impurity emissions, the chord-integrated intensity is estimated by integrating the emission between inner and outer boundaries. The chord-integrated intensity of CIV emissions at the top plasma edge is calculated as a function of horizontal position. It is shown in Fig. 4 (a). The observation chord length calculated at each toroidal position is shown in Fig.4 (b). The local emissivity of CIV is then obtained in dividing the chord-integrated intensity by the chord length. The result is plotted in Fig. 4 (c).

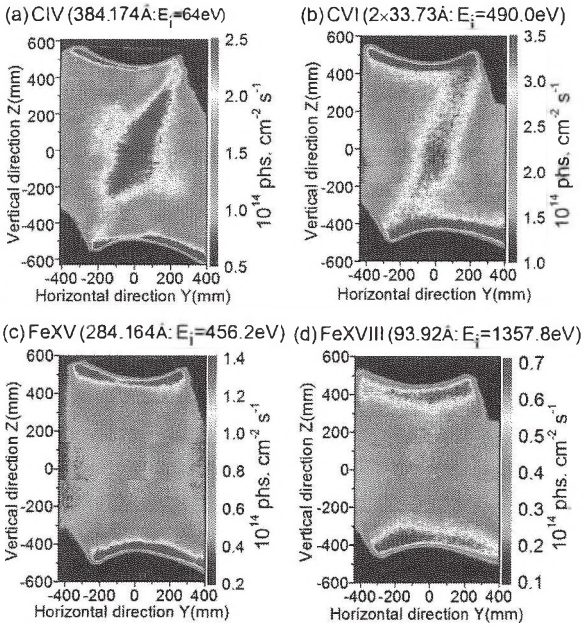

Fig. 2 2-D distributions of (a) CIV, (b) CVI, (c) FeXV and (d) FeXVIII at R_{ax} = 3.60 m.

The poloidal angle at the top plasma edge is calculated for each horizontal position from the assumed magnetic flux surface in the ergodic layer, as shown in Fig. 4 (d). Thus, the poloidal distribution of CIV emissivity near the top edge can be reconstructed from the 2-D CIV distribution with vertical and horizontal coordinates. The poloidal distribution of CIV emissivity near the bottom edge can be also analyzed in the same manner.

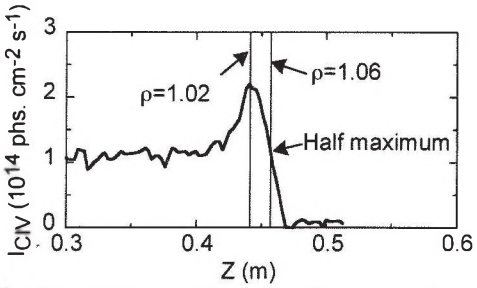

Fig. 3 CIV vertical profile at Y = 0 as a function of vertical position (also see Fig. 2).

4. Results

The poloidal emissivity distribution evaluated from the 2-D distribution in Figs. 2 (a)-(d) is shown in Figs. 5 (a)-(d) as a function of poloidal angles θ_{Top} and θ_{Bottom} at the top and bottom edges, respectively. Here, the poloidal angle is defined by an angle toward counter-clock-wise direction as a reference point of long axis of elliptical plasma shape at outboard side. The poloidal distribution measured at the top and bottom edges is plotted with dashed and solid lines, respectively. Due to a limited observation range of the EUV spectrometer system, the distribution is obtained in ranges of $55° \leq \theta_{Top} \leq 110°$ and $255° \leq \theta_{Bottom} \leq 320°$. The poloidal distribution of these impurity species is also plotted against horizontally elongated plasma cross section. The result shown in Fig. 6 indicates the radial location of impurity ions moves inwardly as the ionization energy increases. Seeing Figs. 5 and 6 it is clear that the poloidal distribution is non-uniform for impurity ions existing in the ergodic layer and in the vicinity of LCFS and the non-uniformity becomes stronger with reduction of the ionization energy of impurity ions. This means impurity ions located in outer region of the ergodic layer exhibit larger non-uniformity in the poloidal distribution. In addition, the emissivity is stronger as the impurity location is close to the X-point, while it is weak at both the top and the bottom O-points defined by poloidal positions of the elliptical plasma boundary adjacent to helical coils.

The emissivity distribution is normalized by emissivity at the bottom O-point, $\theta_{Bottom} = 270°$, to compare the non-uniformity among four impurity species in details. The result is shown in Fig. 7. The normalized poloidal distribution becomes gradually uniform as the radial location of impurity ions moves inside. The

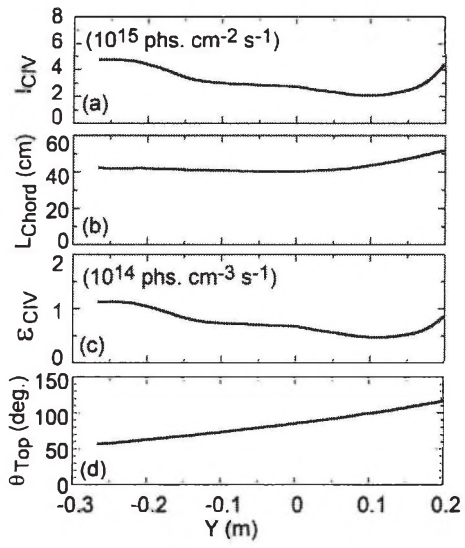

Fig. 4 (a) Chord-integrated intensity of CIV, (b) observation chord length, (c) CIV emissivity and (d) poloidal angle at the top plasma edge as a function of horizontal position, Y.

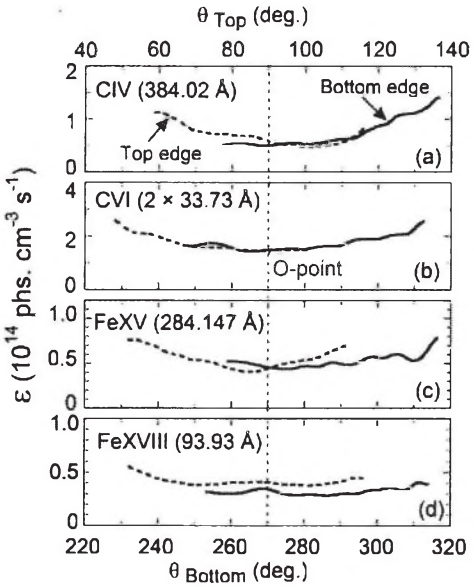

Fig. 5 Poloidal distributions of (a) CIV, (b) CVI, (c) FeXV and (d) FeXVIII as a function of poloidal angles of θ_{Top} and θ_{Bottom}.

poloidal profile of CIV shows an extremely non-uniform distribution. Since the C^{3+} ions with low ionization energy (E_i = 64 eV) is located near the edge boundary in the ergodic layer, the C^{3+} ion is strongly affected by a specific edge impurity transport, which is dominant in the ergodic layer with 3-D magnetic field structure. On the contrary, the poloidal profile of FeXVIII located at $0.78 \leq \rho \leq 0.90$ indicates a relatively flat distribution. This means the FeXVIII emissivity is a function of magnetic surface.

The carbon distribution in the ergodic layer has been also analyzed with a 3-D edge plasma transport code, EMC3-EIRINE [7]. The emissivity distribution of CIV (312.4 Å) simulated with the code is plotted in Fig. 8. This indicates that the CIV emission located in the ergodic layer is stronger when the radial location moves outside. The simulated result well supports our present result, while the estimation of the poloidal distribution is obtained from the 2-D distribution. Therefore, the present analysis can provide a reliable method to evaluate the impurity poloidal distribution.

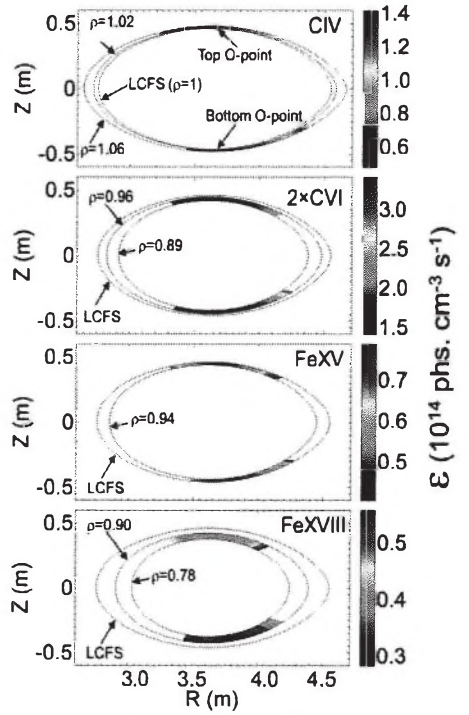

Fig. 6 Poloidal distributions of (a) CIV, (b) CVI, (c) FeXV and (d) FeXVIII at horizontally elongated plasma cross section. The emissivity is expressed in different colors.

5. Summary

The poloidal impurity emissivity distribution of CIV, CVI, FeXV and FeXVIII is reconstructed from the 2-D distribution measured with space-resolved EUV spectrometer system in LHD. A non-uniform poloidal distribution is clearly observed for CIV, while the FeXVIII distribution is basically a function of magnetic surface. The present result for CIV is well supported by the 3-D simulation.

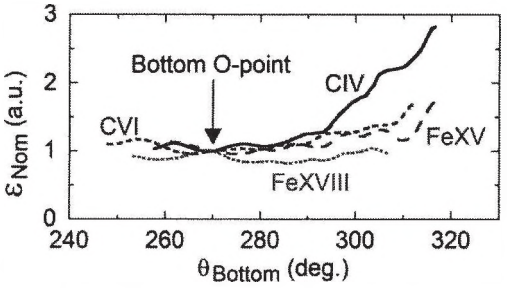

Fig. 7 Emissivity profiles of CIV, CVI, FeXV and FeXVIII normalized at $\theta_{Bottom} = 270°$.

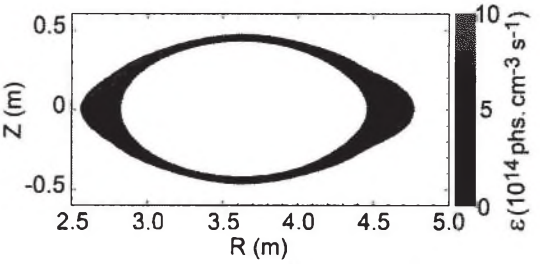

Fig.8 Simulation of emissivity distribution of CIV (312.4Å) using EMC3-EIRINE.

Acknowledgments

The authors thank all members of the LHD Experiment Group for their technical supports. This work was partially carried out under the LHD project financial support (NIFS14ULPP010) and also partly supported by the JSPS-NRF-NSFC A3 Foresight Program in the field of Plasma Physics (NSFC: No.11261140328, NRF: No. 2012K2A2A6000443).

References

[1]. N. Ohyabu, *et al.*, Nucl. Fusion **34**, 387 (1994).
[2]. T. Morisaki, *et al.*, J. Nucl. Mater. **31**, 3548 (2003).
[3]. S. Morita, *et al.*, Nucl. Fusion **53**, 093017 (2013).
[4]. E. H. Wang, *et al.*, Rev. Sci. Instrum. **83**, 043503 (2012).
[5]. S. Morita, *et al.*, Plasma Phys. Control. Fusion **56**, 094007 (2014).
[6]. C. F. Dong, *et al.*, Rev. Sci. Instrum. **83**, 10D509 (2012).
[7]. M. Kobayashi, *et al.*, Nucl. Fusion **53**, 033011 (2013).